Article

Silicon–Nitrogen Bonding in Silatranes: Assignment of Photoelectron Spectra

A. B. Trofimov, V. G. Zakrzewski, O. Dolgounitcheva, J. V. Ortiz, V. F. Sidorkin, E. F. Belogolova, M. Belogolov, and V. A. Pestunovich

J. Am. Chem. Soc., **2005**, 127 (3), 986-995• DOI: 10.1021/ja045667q • Publication Date (Web): 24 December 2004

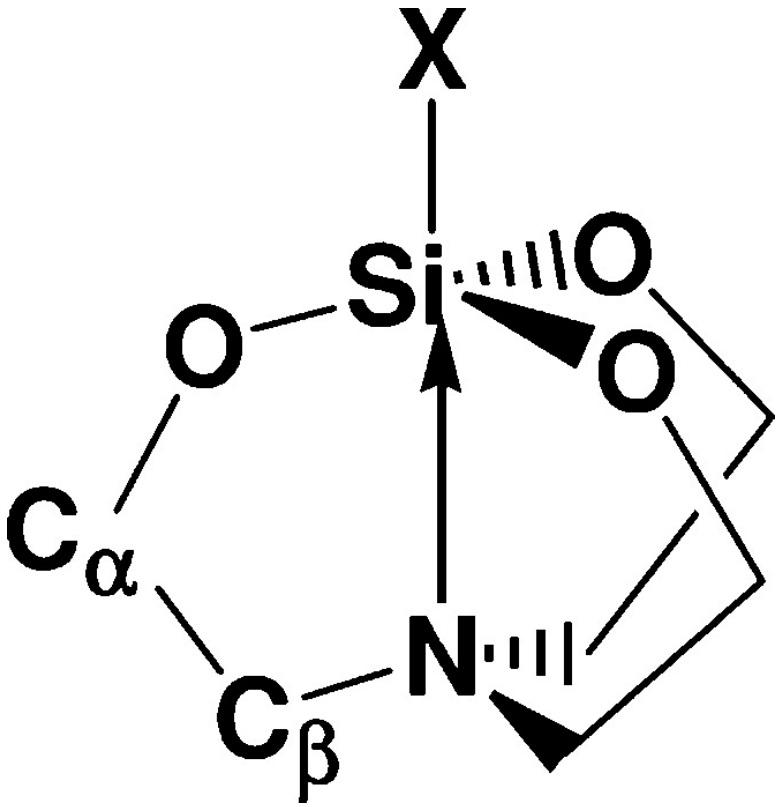

More About This Article

Additional resources and features associated with this article are available within the HTML version:

- Supporting Information
- Links to the 1 articles that cite this article, as of the time of this article download
- Access to high resolution figures
- Links to articles and content related to this article
- Copyright permission to reproduce figures and/or text from this article

J|A|C|S
ARTICLES
Published on Web 12/24/2004

Silicon−Nitrogen Bonding in Silatranes: Assignment of Photoelectron Spectra

A. B. Trofimov,[†] V. G. Zakrzewski,[‡] O. Dolgounitcheva,[‡] J. V. Ortiz,*[,‡]
V. F. Sidorkin,[¶] E. F. Belogolova,[¶] M. Belogolov,[¶] and V. A. Pestunovich[§,¶]

Contribution from the Laboratory of Quantum Chemistry, Computer Center, Irkutsk State University, 664003 Irkutsk, Russian Federation, Department of Chemistry, Kansas State University, Manhattan, Kansas 66506-3701, and A. E. Favorsky Irkutsk Institute of Chemistry, 664033 Irkutsk, Russian Federation

Received July 19, 2004; E-mail: ortiz@ksu.edu

Abstract: Silicon−nitrogen bonding and the photoelectron spectra of hydro−silatrane and methyl−silatrane, $XSi[OCH_2CH_2]_3N$ (X = H and Me), were studied with ab initio electron propagator theory, many-body methods, and density functional models. A linear vibronic coupling (LVC) model was employed to estimate vibrational widths of the ionization bands and to study the dependence of the ionization energies on the molecular geometry. Particular attention was given to coordinates that change the Si−N distance and the strength of the donor−acceptor interaction between these two atoms. The ionization energy of the highest occupied molecular orbital has a very strong geometrical dependence which leads to an unusually large vibrational width in the corresponding photoelectron band. The assignment of this band in methyl−silatrane, which was controversial for a long time, is resolved by the present study. The calculated photoelectron spectra allow for clear assignment of at least three more bands in the observed spectra. The present results demonstrate the important role of electrostatic interactions in Si ← N bonding and in the outer-valence ionization energies of the silatranes.

Introduction

Silatranes are important heterocyclic molecules with interesting physical and chemical properties and a wide range of potential applications.[1−3] These molecules have a cage structure (Figure 1) in which the N-$[CH_2]_3$ and X-Si$[O]_3$ fragments face each other. Since these groups have pronounced donor and acceptor characteristics, their interaction leads to formation of an intramolecular Si ← N donor−acceptor bond. The existence of such a bond in silatranes is firmly established, and these compounds are considered to be examples of systems where silicon is pentacoordinate.[3]

It is believed that the Si ← N bond is responsible for many important properties of silatranes,[1,3] though its characteristics are certainly quite different from those of an ordinary chemical bond. The length of the Si ← N bond in most silatranes depends on the nature of the substituent X and varies in crystals between 1.97 and 2.24 Å. In the gas phase, the length is typically increased by 0.28 Å.[3] This means that the Si ← N bond is longer than the usual Si−N bond (1.7−1.8 Å), but it is distinctly shorter than the sum of the corresponding van der Waals distances (∼3.5 Å).

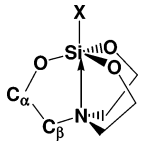

Figure 1. Structure of hydro−silatrane (X = H) and methyl−silatrane (X = Me).

The actual mechanism of Si ← N coordination is far from being understood. Whereas the key role of the N 2p lone pair (LP) here is indisputable, there remain considerable controversies about other aspects of the bonding. In particular, it is unclear whether the N 2p LP is attracted only by the positive charge of the silicon, or if there is also a charge transfer to its unoccupied (3d, 4s, or 4p) atomic orbitals.[1,4] There also is still no agreement about the covalent component of the Si ← N bond, which is predicted by three-center four-electron (3c4e)[5] and dative interaction models.[6]

There is therefore a continuing interest in the electronic and molecular structure of silatranes.[3] This is well reflected by

[†] Irkutsk State University.
[‡] Kansas State University
[¶] A.E. Favorsky Irkutsk Institute of Chemistry.
[§] Deceased.

(1) Voronkov, M. G.; Dyakov, V. M. *Silatranes*; Nauka: Novosibirsk, 1978.
(2) Lukevics, E.; Pudova, O. A.; Sturkovich, R. *Molecular Structure of Organosilicon Compounds*; Ellis Horwood: Chichester, U.K., 1989.
(3) Pestunovich, V.; Kirpichenko, S.; Voronkov, M. In *The Chemistry of Organic Silicon Compounds*; Rappoport, Z., Apeloig, Y., Eds.; Wiley: Chichester, U.K., 1998; Vol. 2.
(4) (a) Voronkov, M. G. *Pure Appl. Chem.* **1996**, *13*, 35. (b) Turley, J. F.; Boer, F. P. *J. Am. Chem. Soc.* **1968**, *90*, 4026. (c) Frye, C. L.; Vincent, G. A.; Finzel, W. A. *J. Am. Chem. Soc.* **1971**, *93*, 6805.
(5) (a) Musher, J. I. *Angew. Chem., Int. Ed. Engl.* **1969**, *8*, 54. (b) Sidorkin, V. F.; Pestunovich, V. A.; Voronkov, M. G. *Dokl. Phys. Chem.* **1977**, 850 (English translation).
(6) Haaland, A. *Angew. Chem., Int. Ed. Engl.* **1989**, *28*, 992.

10.1021/ja045667q CCC: $30.25

experimental[7−14] and theoretical[15−23] work that is relevant for the present study. Much work has been devoted to spectroscopic characterization of the bonding situation in silatranes. In particular, photoelectron spectroscopy was employed to probe the orbital structure and to study trends related to the nature of the substituent at the silicon atom.[7−11] However, attempts to interpret the resulting spectra encountered certain difficulties which could not be fully resolved even with the help of previous theoretical studies.[9−11,24] One such issue concerns the nature of the photoelectron band observed in the energetically lowest part of the silatrane spectra. The band appears as a very broad maximum (e.g., in Me−, CH_2Cl−, and $(CH_2)_3Cl$−silatranes) or shoulder (e.g., in H−, F−, and EtO−silatranes)[7,10] and could not be unambiguously assigned for Me−, F−, and EtO−silatranes. In Me−silatrane, for example, two opposite views on the origin of this band can be found in the literature: (i) the band is due to contamination by impurities (e.g., products of the partial silatrane hydrolysis), that is, it belongs to another substance;[8,11] (ii) the band is due to the ionization of silatranes.[7,9,10,24] Critical analysis of the available data does not allow one to favor one of the two viewpoints, and only a more systematic theoretical study can clarify this fairly complex situation.

In the present work, we study the photoelectron spectra and electronic structure of hydro− and methyl−silatranes (Figure 1) in order to answer at least some of the general questions about silatranes reviewed above. We use the ab initio, outer-valence Green's function (OVGF) approach[25] to compute the energies and spectroscopic factors (intensity coefficients) of the ionization transitions. An important aspect of the present study is that it goes beyond the vertical picture of ionization; we study the geometrical dependence of the ionization energies. In polyatomic molecules, this can be accomplished in a systematic way by using the formalism of a linear vibronic coupling (LVC) model.[26] In addition, the variation of the SiN distance should facilitate improved understanding of the Si ← N bond.

Computational Methods

To obtain information on the vibrational structure of the ionization bands, we employ a linear vibronic coupling (LVC) formalism.[26] This formalism makes use of the vibronic Hamiltonian of the form

$$H = H_0 + E_i + \sum_{s\in a_1} \kappa_s^i Q_s \tag{1}$$

which describes transitions from the 0th vibrational level of the electronic ground state, $|\Psi_0^N\rangle$, into the vibrational manifold of the cationic final state, $|\Psi_i^{N-1}\rangle$. The third term on the right-hand-side of eq 1 arises from a Taylor expansion of the potential energy through linear terms in the totally symmetric (a_1) normal coordinates, Q_s, of the ground state;[27−29] the expansion coefficients, κ_s^i, are the so-called intrastate vibronic coupling constants. H_0 is the vibrational Hamiltonian of the electronic ground state describing noninteracting harmonic oscillators with frequencies ω_s.

$$H_0 = \frac{1}{2}\sum_s \omega_s \left(\frac{\partial^2}{\partial Q_s^{\,2}} + Q_s^{\,2} - 1 \right) \tag{2}$$

In the Hamiltonian H_0, the vibrational ground-state energy is taken as the origin of the energy scale. The coupling constants, κ_s^i, vertical ionization energies (IE), E_i, and frequencies, ω_s, represent parameters of the formalism and have to be determined in a suitable way. Since the corresponding spectral function is of no interest for the present qualitative study, we introduce here only the second spectral moment

$$\Delta_i = 2(2\ln 2)^{1/2} \left(\sum_{s\in a_1} (\kappa_s^i)^2 \right)^{1/2} \tag{3}$$

which can be used as a measure of the vibrational width of the electronic band. The intrastate coupling constants, κ_s^i, entering the above expressions can be determined with the aid of the relation[26]

$$\kappa_s^i = \frac{1}{\sqrt{2}} \left(\frac{\partial E_i}{\partial Q_s} \right)_0 \tag{4}$$

where the derivative of the ionization energy, E_i, with respect to the dimensionless normal coordinates, Q_s, is to be taken at the equilibrium geometry of the electronic ground state. The coupling constants, κ_s^i, were evaluated numerically according to eq 4 by computing the IEs at several nuclear configurations $Q_s' = Q_0 \pm xQ_s$, which were constructed using the ground-state normal coordinates Q_s and the scaling factor $x = 0.5$. In the present work, the Q_s values were computed numerically by performing standard vibrational analysis for the equilibrium molecular geometry.

The ionization energies and spectroscopic factors (pole strengths) were computed using the outer-valence Green's function (OVGF)[25] approximation, as implemented by one of us in the Gaussian suite of programs.[33] Standard analytical-gradient geometry optimizations were

(7) Cradock, S.; Ebsworth, E. A. V.; Muiry, I. B. *J. Chem. Soc., Dalton Trans*. **1975**, 25.
(8) Voronkov, M. G.; Brodskaya, E. I.; Belyaeva, V. V.; Chuvashov, D. D.; Toryashinova, D. D.; Ermikov, A. F.; Baryshok, V. P. *J. Organomet. Chem.* **1986**, *311*, 9.
(9) Brodskaya, E. I.; Voronkov, M. G.; Taryashinova, D. D.; Baryshok, V. P.; Ratovski, G. V.; Chuvashov, D. D.; Efremov, V. G. *J. Organomet. Chem.* **1987**, *336*, 49.
(10) Peel, J. B.; Wang, D. J. J. *J. Chem. Soc., Dalton Trans.* **1988**, 1963.
(11) Sidorkin, V. F.; Balakhchi, G. K. *Struct. Chem.* **1994**, *5*, 187.
(12) Shishkov, I. F.; Khristenko, L. V.; Rudakov, F. M.; Golubinskii, A. B.; Vilkov, L. V.; Karlov, S. S.; Zaitseva, G. S.; Samdal, S. *Struct. Chem.* **2004**, *15*, 11.
(13) Shen, Q.; Hilderbrandt, R. L. *J. Mol. Struct.* **1980**, *64*, 257.
(14) Lyssenko, K. A.; Korlyukov, A. K.; Antipin, M. Yu.; Knyazev, S. P.; Kirin, V. N.; Alexeev, N. V.; Chernyshev, E. A. *Mendeleev Commun.* **2000**, 88.
(15) Milov, A. A.; Minyaev, R. M.; Minkin, V. I. *Zh. Org. Khim.* **2003**, *39*, 372.
(16) Yoshikawa, A.; Gordon, M. S.; Sidorkin, V. F.; Pestunovich, V. A. *Organometallics* **2001**, *20*, 927.
(17) Anglada, J. M.; Bo, C.; Boffil, J. M.; Crehuet, R.; Poblet, J. M. *Organometallics* **1999**, *18*, 5584.
(18) Csonka, G. I.; Hencsei, P. *J. Mol. Struct. (THEOCHEM)* **1996**, *362*, 1996.
(19) Dahl, T.; Skancke, P. N. *Int. J. Quantum Chem.* **1996**, *60*, 567.
(20) Csonka, G. I.; Hencsei, P. *J. Comput. Chem.* **1996**, *17*, 767.
(21) Boggs, J. E.; Peng, C.; Pestunovich, V. A.; Sidorkin, V. F. *J. Mol. Struct. (THEOCHEM)* **1995**, *357*, 67.
(22) Schmidt, M. W.; Windus, T. L.; Gordon, M. S. *J. Am. Chem. Soc.* **1995**, *117*, 7480.
(23) Gordon, M. S.; Carroll, M. T.; Jensen, J. H. *Organometallics* **1991**, *10*, 2657.
(24) Beliaeva, V. V.; Voronkov, M. G. *Zh. Struct. Khim.* **2001**, *42*, 826.
(25) (a) von Niessen, W.; Schirmer, J.; Cederbaum, L. S. *Comput. Phys. Rep.* **1984**, *1*, 57. (b) Zakrzewski, V. G.; von Niessen, W. *J. Comput. Chem.* **1993**, *14*, 13. (c) Zakrzewski, V. G.; Ortiz, J. V. *Int. J. Quantum Chem.* **1995**, *53*, 583. (d) Zakrzewski, V. G.; Ortiz, J. V. *Int. J. Quantum Chem.* **1994**, *S28*, 23.
(26) Köppel, H.; Domcke, W.; Cederbaum, L. S. *Adv. Chem. Phys.* **1984**, *57*, 59.
(27) The dimensionless normal coordinates, Q_s, are obtained from those of Wilson et al. (ref 28) by multiplying with $\sqrt{\omega_s}$ (where ω_s is the ground-state vibrational frequency for mode ν_s).
(28) Wilson, E. B.; Decius, J. C.; Cross, P. C. *Molecular Vibrations*; McGraw-Hill: New York, 1955.
(29) Cederbaum, L. S.; Domcke, W. *Adv. Chem. Phys.* **1977**, *36*, 205.
(30) (a) Cizek, J. *Adv. Chem. Phys.* **1969**, *14*, 35. (b) Purvis, G. D.; Bartlett, R. J. *J. Chem. Phys.* **1982**, *76*, 1910. (c) Scuseria, G. E.; Janssen, C. L.; Schaefer, H. F. *J. Chem. Phys.* **1988**, *89*, 7382.
(31) For example, see: Parr, R. G.; Yang, W. *Density-Functional Theory of Atoms and Molecules*; Oxford University Press: New York, 1989.
(32) (a) Becke, A. D. *J. Chem. Phys.* **1993**, *98*, 5648. (b) Lee, C.; Yang, W.; Parr, R. G. *Phys. Rev. B* **1988**, *37*, 785.

Table 1. Mulliken Populations in the Eight Highest MOs of H−Silatrane[a]

atom	19a	18a	14e	13e	17a	16a	12e	15a
N	0.89	0.34	0.03	0.01	0.01	0.03	0.28	0.01
Si	0.07	0.09	0.06	0.08	0.37	0.18	0.03	0.02
O	0.09	0.32	0.34	0.32	0.18	0.31	0.15	0.09
C_β	0.05	0.03	0.10	0.11	0.07	0.11	0.05	0.06
C_α	0.07	0.03	0.09	0.06	0.01	0.10	0.23	0.25
H(X)	0.14	0.23	0.0	0.0	0.69	0.01	0.0	0.02

[a] HF calculations using the 6-311G** basis for the CCSD molecular geometry. Units are electrons; the sum over all atoms is 2.

Table 2. Mulliken Populations in the Eight Highest MOs of Me−Silatrane[a]

atom	21a	20a	15e	19a	14e	18a	13e	17a	12e
N	1.03	0.23	0.03	0.0	0.01	0.06	0.09	0.01	0.20
Si	0.07	0.20	0.05	0.24	0.09	0.15	0.0	0.01	0.04
O	0.05	0.24	0.35	0.25	0.31	0.34	0.04	0.08	0.12
C_β	0.06	0.03	0.09	0.06	0.11	0.11	0.03	0.06	0.02
C_α	0.07	0.02	0.09	0.02	0.05	0.08	0.07	0.26	0.16
C(X)	0.09	0.53	0.02	0.46	0.0	0.0	0.71	0.01	0.30

[a] See the footnote of Table 1.

employed to obtain parameters of the ground-state molecular structure. Preliminary optimizations with second-order Møller−Plesset perturbation theory (MP2) were refined using the coupled-cluster singles and doubles (CCSD) approach.[30] Separate optimizations and harmonic frequency calculations were based on density functional theory (DFT)[31] and the B3LYP potential.[32] In all cases, no symmetry constraints were used in the geometry optimization. The K-shell orbitals of C, N, and O, as well as the K- and L-shell orbitals of Si, were kept frozen in all CCSD, MP2, and OVGF calculations. These calculations were performed using the GAUSSIAN program package.[33] Three-dimensional plots of the orbital amplitudes were generated using the MOLDEN program.[34]

The 6-31G* double-ζ plus polarization basis set[35] was used in the MP2 and CCSD calculations, whereas the 6-311G* triple-ζ basis[36] was employed in the B3LYP computations. The OVGF calculations of vertical ionization energies were performed for the series of basis sets comprising 6-31G*, 6-31G**, 6-311G**, and 6-311G(2df,p) bases.

Results and Discussion

The ground-state Hartree−Fock (HF) electronic configuration of H− and Me−silatranes (C_3 point group), as obtained from the present calculations, may be written respectively as

(core) (inner-valence)

$12a^2 8e^4 13a^2 9e^4 10e^4 14a^2 11e^4 15a^2 12e^4 16a^2 17a^2 13e^4 14e^4 18a^2 19a^2$

and

(core) (inner-valence)

$14a^2 8e^4 15a^2 9e^4 10e^4 16a^2 11e^4 12e^4 17a^2 13e^4 18a^2 14e^4 19a^2 15e^4 20a^2 21a^2$

where only the outer-valence part of the configuration is shown explicitly. Several outermost molecular orbitals (MO) of these molecules can be satisfactorily interpreted using the results of the Mulliken population analysis in Tables 1 and 2.[37,38] In both molecules, the highest occupied MO (HOMO) exhibits a large N 2p LP component, but it also is widely delocalized over the entire molecule (Figure 2). The group of six MOs (18a, 14e, 13e, and 16a in H−silatrane and 20a, 15e, 14e, and 18a in Me−silatrane) is related to the LPs of oxygens. Orbital 17a in

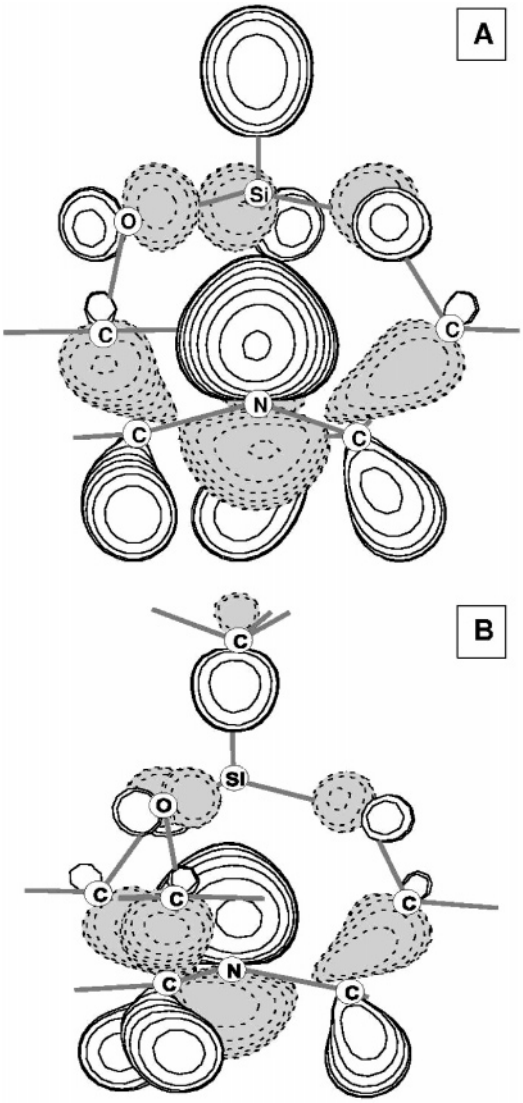

Figure 2. N 2p LP molecular orbitals of hydro−silatrane (A) and methyl−silatrane (B).

(33) Frisch, M. J.; Trucks, G. W.; Schlegel, H. B.; Scuseria, G. E.; Robb, M. A.; Cheeseman, J. R.; Montgomery, J. A., Jr.; Vreven, T.; Kudin, K. N.; Burant, J. C.; Millam, J. M.; Iyengar, S. S.; Tomasi, J.; Barone, V.; Mennucci, B.; Cossi, M.; Scalmani, G.; Rega, N.; Petersson, G. A.; Nakatsuji, H.; Hada, M.; Ehara, M.; Toyota, K.; Fukuda, R.; Hasegawa, J.; Ishida, M.; Nakajima, T.; Honda, Y.; Kitao, O.; Nakai, H.; Klene, M.; Li, X.; Knox, J. E.; Hratchian, H. P.; Cross, J. B.; Adamo, C.; Jaramillo, J.; Gomperts, R.; Stratmann, R. E.; Yazyev, O.; Austin, A. J.; Cammi, R.; Pomelli, C.; Ochterski, J. W.; Ayala, P. Y.; Morokuma, K.; Voth, G. A.; Salvador, P.; Dannenberg, J. J.; Zakrzewski, V. G.; Dapprich, S.; Daniels, A. D.; Strain, M. C.; Farkas, O.; Malick, D. K.; Rabuck, A. D.; Raghavachari, K.; Foresman, J. B.; Ortiz, J. V.; Cui, Q.; Baboul, A. G.; Clifford, S.; Cioslowski, J.; Stefanov, B. B.; Liu, G.; Liashenko, A.; Piskorz, P.; Komaromi, I.; Martin, R. L.; Fox, D. J.; Keith, T.; Al-Laham, M. A.; Peng, C. Y.; Nanayakkara, A.; Challacombe, M.; Gill, P. M. W.; Johnson, B.; Chen, W.; Wong, M. W.; Gonzalez, C.; Pople, J. A. *Gaussian 03*, revision B.03; Gaussian, Inc.: Pittsburgh, PA, 2003.
(34) Schaftenaar, G. *MOLDEN 3.4*, CAOS/CAMM Center: The Netherlands, 1998.
(35) (a) Hehre, W. J.; Ditchfield, R.; Pople, J. A. *J. Chem. Phys.* **1972**, *56*, 2257. (b) Hariharan, P. C.; Pople, J. A. *Theor. Chim. Acta* **1973**, *28*, 213. (c) Francl, M. M.; Pietro, W. J.; Hehre, W. J.; Binkley, J. S.; Gordon, M. S.; DeFrees, D. J.; Pople, J. A. *J. Chem. Phys.* **1982**, *77*, 3654.
(36) Krishnan, R.; Binkley, J. S.; Seeger, R.; Pople, J. A. *J. Chem. Phys.* **1980**, *72*, 650.
(37) The Hartree−Fock orbital Mulliken population analysis was performed using the GAMESS program package (ref 38).
(38) Schmidt, M. W.; Baldridge, K. K.; Boatz, J. A.; Elbert, S. T.; Gordon, M. S.; Jensen, J. H.; Koseki, S.; Matsunaga, N.; Nguyen, K. A.; Su, S.; Windus, T. L.; Dupuis, M.; Montgomery, J. A. *J. Comput. Chem.* **1993**, *14*, 1347.

Table 3. MP2/6-31G*, B3LYP/6-311G*, and CCSD/6-31G* Optimized Geometrical Parameters[a]

	H–Silatrane (X = H)				Me–Silatrane (X = Me)			
	MP2	DFT	CCSD	exp[b]	MP2	DFT	CCSD	exp[c]
Si−N	2.30	2.57	2.39	2.41	2.39	2.70	2.52	2.45
Si−X[d]	1.47	1.47	1.48		1.86	1.86	1.86	
Si−O	1.69	1.67	1.68	1.65	1.69	1.67	1.68	1.66
O−C_β	1.41	1.41	1.41	1.40	1.41	1.41	1.42	1.41
C_α−C_β	1.52	1.53	1.53	1.50	1.52	1.54	1.53	1.56
C_α−N	1.46	1.46	1.46	1.44	1.46	1.45	1.45	1.46
XSiO	99.4	103.2	101.0	101.2	101.3	105.6	103.4	100.9
SiOC_β	122.0	125.0	122.9	128.1	122.3	125.4	123.2	127.0
O$C_\beta C_\alpha$	108.8	110.5	106.8	117.0	109.0	111.0	109.6	116.4
$C_\beta C_\alpha$N	108.9	106.3	106.8	108.2	106.5	110.0	107.3	106.7
$C_\alpha NC_\alpha$	114.7	117.6	115.6	113.2	115.3	118.5	116.6	114.7

[a] Bond lengths are in angstroms, angles are in degrees. [b] Gas-phase electron diffraction measurements (ref 12). [c] Gas-phase electron diffraction measurements (ref 13). [d] Methyl group is in a skewed configuration with respect to the X−Si[−O−]$_3$ fragment.

H−silatrane (19a in Me−silatrane) is the σ (Si−X) bonding MO. The deeper MOs are more delocalized and describe various σ-bonds among Si, C, O, N, and H atoms.

Ground-State Geometry. The results of the present ground-state geometry optimizations for H− and Me−silatranes are shown in Table 3. Both molecules are predicted to have a symmetric C_3 configuration in which the Si−N−C_α−C_β−O cyclic fragments have a nonplanar structure due to an out-of-plane position of the C_β atom.

The data in Table 3 reflect difficulties in the theoretical treatment of the silatrane molecules. As can be seen, the methods used in the calculations yield very different results. The Si−N bond lengths predicted by the MP2 and B3LYP treatments differ by about 0.3 Å. Compared to those in the gas phase, experimental Si−N distances in H− and Me−silatranes (2.41 and 2.45 Å, respectively),[12,13] the present B3LYP distances (2.57 and 2.70 Å, respectively) are grossly overestimated. At the same time, the present MP2 distances (2.30 and 2.39 Å, respectively) look more reasonable, albeit too low. Strong disagreement between the MP2 and B3LYP results can be seen also for the other parameters dependent on the Si−N distance. For example, the bond angles in the Si−N−C_α−C_β−O cycles differ by up to 3°. Parameters independent of the Si−N distance, on the other hand, are less sensitive to the theoretical treatment and are nearly the same in both molecules. Similar trends for the DFT and MP2 geometries of various silatranes also can be found in previous theoretical work.[15−18,20]

Because of the disagreements between the MP2 and B3LYP results, we had to carry out additional geometry optimization using the more accurate CCSD approach. As expected, the CCSD results (Table 3) for H−silatrane agree very well with the experimental data. Distinct improvement with respect to MP2 can be seen for the Si−N distance. Interestingly, no obvious improvement for this parameter was obtained at the CCSD level in Me−silatrane. In this molecule, CCSD overestimates the Si−N distance by the same amount (0.06−0.07 Å) as MP2 underestimates it. Here, however, one has to take into account the very flat shape of the ground-state potential energy surface along the Si−N coordinate.[3] In our calculations, this flatness is confirmed by the course of the B3LYP optimizations, which were started from the MP2 geometries. Here, the total ground-state energies of the H− and Me−silatranes changed by 1.6 and 2.2 kcal/mol, respectively, whereas the Si−N bonds increased by about 0.3 Å. The flat ground-state potential should clearly not only complicate theoretical treatments of silatranes, as first noted by Schmidt et al.,[22] but also affect experimental measurements, making them sensitive to the phase state,[23] temperature, and other factors.[20] The accuracy of the experimental data in Table 3 may be questioned in view of the surprising similarity of the Si−N distances in H− and Me−silatrane, which differ only by 0.04 Å. The differences predicted by the theoretical methods in Table 3 are consistently larger (0.09−0.13 Å). Also, distinctly longer Si−N distances in Me−silatrane than in H−silatrane can be expected from chemical considerations based on the stronger inductive effect of the methyl group.

Table 4. Vertical Ionization Energies (E, eV) and Spectroscopic Factors (P) for H-silatrane

	HF[a]	OVGF[a]		Exp[b]	OVGF[c]			
MO	*E*	*E*	*P*	*E*	*E*[d]	*E*[e]	*E*[f]	*E*[g]
19a	10.76	9.38	0.91		9.68	9.68	9.54	9.38
18a	11.76	10.28	0.91	10.1	10.36	10.30	10.19	10.05
14e	11.98	10.55	0.91	10.4	10.64	10.56	10.49	10.36
17a	12.68	11.72	0.92		11.54	11.49	11.39	11.22
13e	12.75	11.35	0.91	11.2	11.40	11.35	11.28	11.15
16a	13.71	12.25	0.90		12.24	12.22	12.16	12.04
12e	14.36	13.00	0.91		13.02	13.04	12.95	12.80
15a	14.75	13.49	0.91		13.57	13.61	13.53	13.36
11e	15.77	14.43	0.91		14.44	14.45	14.39	14.26
14a	16.67	15.34	0.91		15.25	15.26	15.21	15.12
10e	16.80	15.12	0.90		15.02	15.03	15.12	15.00
9e	17.70	16.20	0.90		16.06	16.09	16.02	15.95
13a	18.38	16.80	0.90		16.71	16.75	16.68	16.60
8e	18.87	17.30	0.90		17.24	17.29	17.22	17.14
12a	19.81	17.85	0.89		17.71	17.78	17.71	17.64

[a] Basis set 6-311G** results at CCSD/6-31G* geometry. [b] Vertical ionization energies are measured as band maxima or shoulder peaks (ref 7). [c] Results at MP2/6-31G* geometry. [d] With the 6-311G(2df,p) basis. [e] With the 6-311G** basis. [f] With the 6-31G** basis. [g] With the 6-31G* basis.

Table 5. Vertical Ionization Energies (*E*, eV) and Spectroscopic Factors (*P*) for Me−Silatrane

	HF[a]	OVGF[a]		Exp[b]	OVGF[c]			
MO	*E*	*E*	*P*	*E*	*E*[d]	*E*[e]	*E*[f]	*E*[g]
21a	10.29	8.86	0.90	8.5	9.25	9.24	9.07	8.92
20a	11.51	10.11	0.90	9.8	10.15	10.10	9.94	9.80
15e	11.85	10.39	0.91	10.2	10.48	10.41	10.32	10.19
19a	12.47	11.16	0.91	11.0	10.95	10.89	10.78	10.65
14e	12.66	11.26	0.91		11.30	11.25	11.17	11.03
18a	13.68	12.16	0.90	12.1	12.14	12.11	12.04	11.92
13e	13.91	12.94	0.91	12.6	12.89	12.88	12.75	12.58
12e	14.38	13.13	0.91	12.9	13.08	13.07	12.96	12.81
17a	14.54	13.27	0.91		13.38	13.42	13.33	13.16
11e	15.68	14.34	0.90	14.0	14.38	14.39	14.32	14.18
16a	16.39	15.04	0.90	14.7	15.12	15.13	15.06	14.92
10e	16.67	14.96	0.90		15.06	15.06	14.98	14.86
9e	17.66	16.14	0.90		15.99	16.02	15.94	15.87
15a	18.15	16.52	0.90		16.44	16.48	16.40	16.32
8e	18.72	17.15	0.90		17.10	17.15	17.07	16.99
14a	19.53	17.55	0.89		17.40	17.46	17.38	17.31

[a] Basis set 6-311G** results at CCSD/6-31G* geometry. [b] Vertical ionization energies are measured as band maxima or shoulder peaks (ref 10). [c] Results at MP2/6-31G* geometry. [d] With the 6-311G(2df,p) basis. [e] With the 6-311G** basis. [f] With the 6-31G** basis. [g] With the 6-31G* basis.

Vertical Ionization Energies. The results of the present OVGF calculations for H− and Me−silatranes are shown in Tables 4 and 5, respectively. As can be seen, the OVGF vertical ionization energies for the CCSD geometry are about 1.4 eV

below the HF values. The maximal OVGF correction does not exceed 2 eV, which suggests the absence of strong electron correlation or orbital relaxation effects. The orbital spectroscopic factors of about 0.9 also support this suggestion and indicate that for H− and Me−silatranes, the one-electron picture of ionization[39] should be valid in the entire outer-valence region.

The experimental vertical ionization energies were determined for Me−silatrane by Peel et al.[10] (Table 5). Discrepancies with experiment at the CCSD geometry are less than 0.4 eV; somewhat better agreement is usually obtained for vertical OVGF predictions on typical organic molecules.[25]

It follows from our basis set study in Tables 4 and 5 that the extension of the basis from 6-31G* to 6-31G** and further to 6-311G** increases the OVGF IEs on the average by about 0.1 eV at each stage. The average energy change due to further d- and f-polarization functions in the 6-311G(2df,p) basis is 0.03 eV. The two outermost MOs seem to be somewhat more sensitive toward modification of the basis than the other MOs. A small and nearly uniform basis set effect, similar to that found here, usually has little or no influence on the qualitative picture of ionization. Thus, a successful assignment of the experimental spectra of silatranes should be possible using a wide range of basis sets. To be on the safe side, in "Assignment of Photoelectron Spectra", we use for this purpose our OVGF results for the 6-311G** basis and the CCSD molecular geometry.

Comparison of the OVGF/6-311G** results for the CCSD and MP2 geometries reveals discrepancies of about 0.3−0.4 eV in the ionization energies of the N 2p LP and Si−X MOs. At the same time, the IEs of the other orbitals do not differ by more than 0.1 eV for the two sets of geometrical parameters. The larger geometrical effect in the case of the N 2p LP and Si−X MOs is especially significant, for it suggests strong nuclear relaxation and increased vibrational width in the corresponding photoelectron bands. The latter factors, being important for correct assignment of the experimental spectra, are analyzed in the next section.

Geometrical Dependence of Ionization Energies. As can be seen from eq 4, the vibronic coupling constants, κ, reflect the dependence of the IEs on the totally symmetric normal coordinates. In Tables 6 and 7, we list the κ constants for the eight and nine outermost MOs of H− and Me−silatranes, respectively (the constants for the deeper MOs are not shown since they are less informative). The totally symmetric modes in Tables 6 and 7 are numbered according to their positions in the full list of normal modes, ordered with respect to their frequencies. To keep the computational effort reasonably low, we determined the κ parameters using HF ionization energies and B3LYP normal coordinates (the 6-311G* basis was employed). This level of approximation provides reasonably accurate κ values. The validity of the approximation is exemplified by the data of Table 8, where the HF and OVGF κ values are compared for two selected MOs and normal modes. Of course, the reliability of the present B3LYP vibrational coordinates and frequencies can be questioned in the view of the B3LYP error for the ground-state geometry (Table 3), but this should not influence the conclusions of our study.

In both molecules, very large coupling constants can be seen for the N 2p LP MOs along the ν_1 and ν_4 normal modes. These modes describe simultaneous stretching of the Si−N bond with some twisting of the X−Si−O_3 and −N[−CH_{2-}]$_3$ fragments about the Si−N axis. Additional large κ values for the N 2p LP MOs are found along the mode ν_{27} of H−silatrane and the analogous mode ν_{31} of Me−silatrane. These modes describe stretchings of the N−C_α and C_α−C_β bonds, which also influence the Si−N distance. These data show that, in particular, the Si−N stretching motion will be strongly excited upon ionization of the N 2p LP electrons. When the sign of the coupling constants and the normal coordinate phase factors are taken into account,

Table 6. HF Linear Vibronic Coupling Constants, $\kappa \times 10$ (eV), for the Eight Lowest Ionization Transitions of H−Silatrane Evaluated with Respect to the Totally Symmetric Normal Modes, ν_n, Frequencies, ω (cm^{-1}), and the Corresponding Vibrational Widths, Δ (eV)

ν_n	ω	19a	18a	14e	13e	17a	16a	12e	15a
1	83	−1.73	0.26	0.0	0.0	1.42	0.63	−0.16	−0.64
4	206	1.96	−0.41	0.0	0.0	−0.81	−0.50	0.13	−0.26
7	293	0.49	0.23	0.18	0.0	0.29	−0.24	0.0	0.50
12	477	0.47	0.0	−0.36	−0.20	0.49	−0.13	−0.26	−0.37
13	569	0.58	0.28	0.22	0.26	−0.52	0.50	0.52	0.47
16	636	−0.23	0.17	−0.22	−0.27	1.09	−0.46	−0.52	-−0.30
17	752	−0.19	0.27	0.36	0.33	0.0	0.38	0.60	−0.23
22	895	−0.72	0.23	0.0	−0.23	0.68	0.34	0.32	0.16
27	1005	1.15	0.0	0.13	0.12	−0.21	0.0	−0.57	0.15
30	1103	−0.71	0.0	0.0	0.0	0.47	−0.56	0.18	0.61
33	1157	0.0	−0.39	0.94	0.86	−1.69	0.89	0.0	00
36	1272	0.28	0.12	0.0	0.23	0.34	0.29	0.0	−0.11
39	1297	−0.22	−0.11	0.19	0.15	0.29	0.40	0.0	−0.40
44	1400	−0.14	−0.19	0.41	0.17	−0.17	0.30	−0.75	−0.14
45	1412	−0.58	0.48	0.0	0.40	0.80	0.0	−0.64	−0.53
50	1510	−0.56	0.0	0.0	−0.12	0.19	0.0	0.22	1.24
53	1535	−0.44	0.13	−0.25	0.33	−0.23	−0.21	−0.14	0.71
54	2308	0.23	−0.48	0.32	0.32	−2.75	0.11	0.29	0.0
57	2988	0.17	−0.22	−0.31	−0.36	−0.17	−0.27	0.18	0.73
60	3011	−0.25	0.0	0.16	0.52	0.0	−0.23	0.0	0.43
63	3072	0.0	−0.14	0.0	0.13	−0.29	0.43	−0.31	−0.96
64	3086	0.38	0.15	0.0	0.0	0.13	−0.20	−0.63	−1.72
Δ		0.79	0.27	0.32	0.34	0.96	0.43	0.42	0.73

Table 7. HF Linear Vibronic Coupling Constants, $\kappa \times 10$ (eV), for the Eight Lowest Ionization Transitions of Me−Silatrane Evaluated with Respect to the Totally Symmetric Normal Modes, ν_n, Frequencies, ω (cm^{-1}), and the Corresponding Vibrational Widths, Δ (eV)

ν_n	ω	21a	20a	15e	19a	14e	18a	13e	17a	12e
1	89	−1.50	0.30	0.0	0.82	0.0	0.48	0.30	−0.14	0.37
5	192	1.54	−0.49	0.0	−0.33	0.0	−0.43	−0.23	−0.26	−0.34
10	292	0.37	0.11	0.20	0.54	0.0	−0.18	−0.12	0.21	−0.10
15	438	0.46	0.0	−0.40	0.0	−0.28	−0.47	0.0	−0.23	0.0
16	552	0.49	0.22	0.20	−0.30	0.22	0.67	0.11	0.34	0.0
19	600	0.13	0.0	0.0	0.0	0.0	−0.19	0.0	0.0	−0.13
22	742	−0.37	0.47	0.12	0.60	0.0	0.24	0.34	0.0	0.51
23	779	−0.32	0.52	−0.61	0.46	−0.52	−0.76	0.0	0.0	0.47
26	888	−0.70	0.38	0.0	0.32	−0.31	0.0	0.44	0.27	0.45
31	1001	1.01	0.0	0.15	−0.12	0.0	0.0	−0.40	0.0	−0.17
34	1102	−0.69	0.0	0.0	0.44	0.0	−0.47	0.0	0.41	0.0
37	1156	0.32	−0.61	0.90	−0.21	0.91	0.75	−0.53	−0.22	−0.64
40	1273	−0.26	0.0	0.0	−0.46	−0.21	−0.27	0.0	0.0	0.13
43	1298	0.0	0.0	0.22	0.0	0.0	0.49	0.0	−0.17	0.16
44	1333	0.0	−1.48	0.13	−1.19	0.10	0.0	0.92	0.53	1.19
49	1402	0.0	−0.16	0.40	−0.12	0.0	0.0	−0.43	−0.19	−0.25
50	1416	−0.62	0.42	0.0	0.60	0.43	0.14	−0.36	−0.39	−0.11
57	1508	−0.60	0.0	0.13	0.20	−0.13	−0.18	0.17	0.83	0.22
58	1530	0.21	0.0	0.12	−0.18	0.0	0.0	0.11	−0.15	0.0
60	1532	−0.38	0.0	−0.26	0.0	0.29	0.0	−0.19	0.27	0.0
63	2973	0.0	−0.19	−0.29	−0.20	−0.31	−0.31	0.0	0.45	0.0
66	3011	−0.29	0.0	0.16	0.17	0.66	−0.10	0.0	0.13	−0.17
67	3040	0.0	−0.20	0.0	−0.14	0.0	0.0	1.28	0.60	1.71
70	3066	0.0	−0.13	0.0	−0.32	0.0	0.50	−0.23	−0.78	−0.27
71	3081	0.38	0.13	0.0	0.14	0.0	−0.12	−0.36	−1.03	−0.26
Δ		0.71	0.47	0.33	0.50	0.37	0.43	0.48	0.49	0.60

(39) Cederbaum, L. S.; Domcke, W.; Schirmer, J.; von Niessen, W. *Adv. Chem. Phys.* **1986**, *65*, 115.

Table 8. Comparison of HF and OVGF Linear Vibronic Coupling Constants $\kappa \times 10$ (eV) in H- and Me-silatranes

molecule	ν_n	method	HOMO[a]	HOMO-1[b]
H−silatrane	ν_1	HF	−1.73	0.26
		OVGF	−1.70	0.38
	ν_4	HF	1.96	−0.41
		OVGF	1.98	−0.26
Me−silatrane	ν_1	HF	−1.50	0.30
		OVGF	−1.43	0.31
	ν_5	HF	1.54	−0.49
		OVGF	1.50	−0.35

[a] With 19a in H−silatrane and 21a in Me−silatrane. [b] With 18a in H−silatrane and 20a in Me−silatrane.

one sees that the N 2p LP IE decreases as the Si−N separation increases. This implies that the Si−N distance in the cations is longer than that in the neutral molecules.

Large coupling constants are obtained also for the Si−X bonding MOs. As could be expected, the largest κ values here occur for stretching vibrations of the Si−X bond (modes ν_{54} and ν_{44} in H− and Me−silatrane, respectively). Interestingly, quite appreciable coupling constants can be seen for the ν_1 and ν_4 modes. This indicates that the displacement of the nitrogen atom in some way influences also the IEs of the Si−X bonding MOs. Since all coupling constants here have opposite signs compared to the N 2p LP case, the opposite behavior of the IEs with respect to changes of the Si−N distance is predicted.

The oxygen LP orbitals, 14e, 13e, and 16a of H−silatrane and 15e, 14e, and 18a of Me−silatrane, have large coupling constants for the normal modes describing alternate O−C_β and O−Si stretching vibrations (ν_{33} and ν_{37} in H− and Me−silatrane, respectively). This demonstrates that, although the above orbitals are largely nonbonding, their energies nevertheless depend on the position of the oxygen and the neighboring atoms. The remaining O 2p LP orbitals (18a in H−silatrane and 20a in Me−silatrane) have distinctly different coupling patterns, which also change from one molecule to the other.

The net effect of the totally symmetric vibrations on the IEs can be seen from the vibrational width parameter Δ (eq 3). The present Δ values for the N 2p LP levels of H− and Me−silatrane (0.79 and 0.71 eV, respectively) imply very broad photoelectron bands. For these bands, it may be difficult to observe the actual vibrational structure due to the small frequencies of the ν_1 modes (83 cm^{-1} in H−silatrane and 89 cm^{-1} in Me−silatrane), which are predominantly active here. The appearance of the bands thus may be somewhat diffuse. From the large coupling constants and small vibrational frequencies obtained here, one can expect that the adiabatic (0−0) IEs will be substantially lower than the vertical IEs, and the spectral intensities of the 0−0 transitions will be small.[26] Also, in such a situation, positions of the N 2p LP band maxima may not exactly match vertical IEs for these transitions. The latter applies to the vertical IEs of Cradock et al.[7] and Peel et al.[10] in Table 5, which were derived as band maxima or shoulder peaks.

The present results also predict large vibrational widths for the photoelectron bands of the Si−X MOs. Here, Δ values of 0.96 and 0.50 eV were obtained for H− and Me−silatrane, respectively. By contrast, the photoelectron bands of the O 2p LP levels characterized by the Δ values of 0.3−0.4 eV are expected to be sharper.

Assignment of Photoelectron Spectra. In Figures 3 and 4, we compare the present theoretical results with the experimental

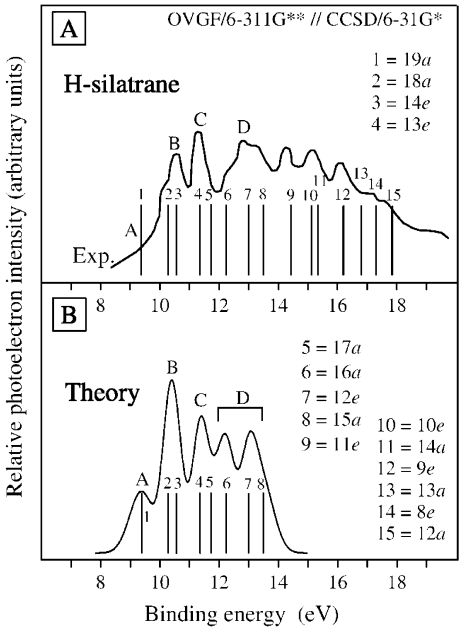

Figure 3. (A) Outer-valence shell photoelectron spectrum of hydro−silatrane.[7] The bar spectrum represents the results obtained using the OVGF approach. (B) Theoretical photoelectron spectrum obtained by combining the OVGF results with the vibrational widths of the electronic transitions estimated using the LVC approach (see text for details).

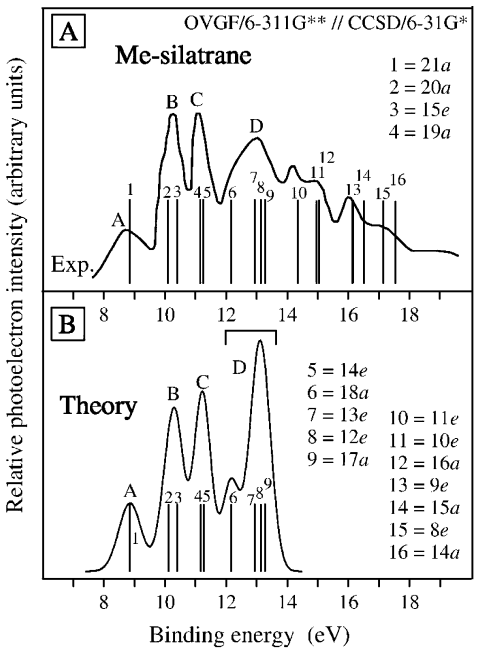

Figure 4. (A) Outer-valence shell photoelectron spectrum of methyl−silatrane.[7] The bar spectrum represents the results obtained using the OVGF approach. (B) Theoretical photoelectron spectrum obtained by combining the OVGF results with the vibrational widths of the electronic transitions estimated using the LVC approach (see text for details).

photoelectron spectra of H− and Me−silatranes.[7] In the A panels, the present OVGF vertical ionization spectra (shown with the bars) are superimposed over the experimental spectral profiles. In the B panels, we show also the theoretical photoionization envelopes, which were obtained by convoluting the vertical OVGF spectra with two types of Gaussian functions. The functions of the first type approximate the experimental resolution and have a fwhm (full width at half-maximum) of

0.5 eV for all transitions. The functions of the second type account for the individual vibrational width of the transitions and have a fwhm equal to their vibrational width parameters, Δ_i, as discussed in "Geometrical Dependence of Ionization Energies".

As seen from Figures 3A and 4A, the present theoretical results agree well with the experimental spectra. The calculated transitions at the lower energies match the major features of the experimental envelopes, so that the maxima A−D of the experimental spectra can be reliably assigned. The feature A represented by a shoulder in the spectrum of H−silatrane and by a maximum in the spectrum of Me−silatrane clearly results from the ionization of a N 2p LP electron. Peak B in both cases is built from two transitions representing ionization from O 2p LP levels (orbitals 18a and 14e in H−silatrane and 20a and 15e in Me−silatrane). Peak C also comprises two transitions, one of them representing ionization from an O 2p LP level (MOs 13e in H−silatrane and 14e in Me−silatrane), while the other one represents ionization from the Si−X orbitals (MOs 17a in H−silatrane and 19a in Me−silatrane). D maxima have a more complex structure, comprising three and four transitions in H− and Me−silatrane, respectively. In each molecule, one of these transitions is due to the ionization from an O 2p LP level (MOs 16a in H−silatrane and 18a in Me−silatrane), whereas the remaining transitions represent ionizations from deeper σ-levels. Preliminary calculations with a method that is designed to treat stronger correlation effects in final states, ADC(3),[25,40] indicate that the spectra become more complex at higher energy due to the increased density of transitions, and their unambiguous assignment is not possible.

The purely energetic considerations used so far do not explain the shape of the observed spectral envelopes. On the other hand, the latter information would be very desirable to confirm our assignments. This is particularly important for the experimental A bands, which were assigned above according to the vertical ionization energies of the N 2p LP of the silatranes. In the past, the strikingly broad appearance of this band in the spectrum of Me−silatrane together with its somewhat different (low energy) location compared to the spectra of the other silatranes gave rise to significant controversies about its assignment.[7−11,24] It was suggested that the lowest photoelectron band in the spectrum of Me−silatrane originates from a different compound.[8,11] In the work of Sidorkin et al.,[11] such an assignment was supported by an observation that nearly all samples of the investigated silatranes were contaminated with products of their incomplete hydrolysis, and that the spectral intensity in the relevant energy range varies with the concentration of these products. The present theoretical envelope in Figure 4B, however, shows clearly that this band is primarily a genuine N 2p LP silatrane band with increased vibrational width. Of course, a certain part of its experimental intensity may indeed come from contaminating products, as observed by Sidorkin et al.,[11] but this does not contradict the present assignment. The calculated theoretical profiles qualitatively reproduce the appearance of the A band in both molecules. In H−silatrane, the band merges with spectral bands at higher energy, giving rise to a low-energy shoulder. The latter is not very pronounced in the experimental spectrum, but the steady growth of the photoelectron intensity between 8 and 10 eV gives clear evidence for an underlying electronic transition.

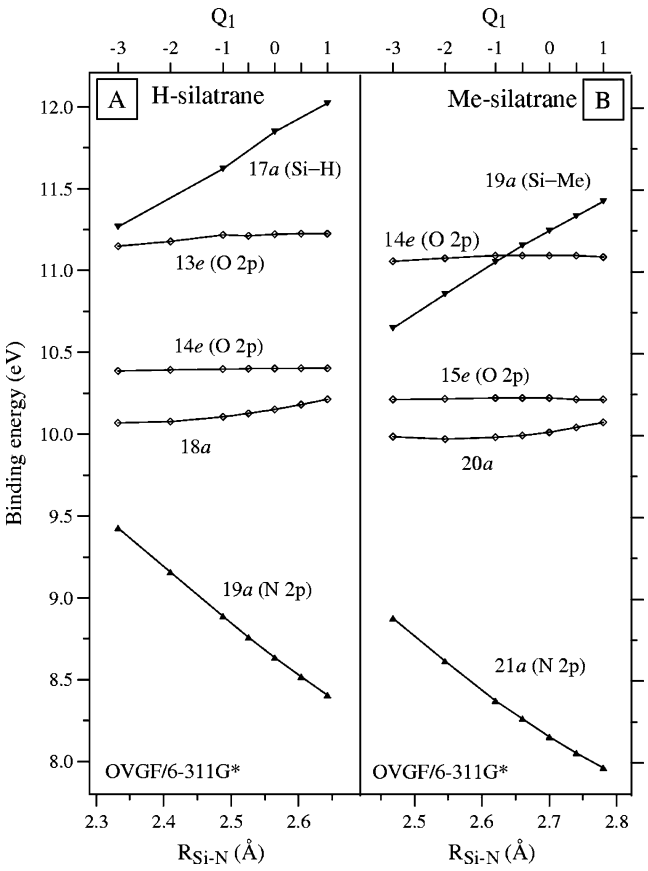

Figure 5. OVGF ionization energies of hydro−silatrane (A) and methyl−silatrane (B) as functions of the Q_1 normal coordinate describing variation of the Si−N distance.

The present theoretical spectra also qualitatively reproduce other features of the experimental spectra up to about 14 eV. In this energy region, our calculations predict, in agreement with experiment, distinct peaks B, C, and D.

Relative intensities and shapes of the spectral peaks in the theoretical spectra in Figures 3B and 4B may not be fully correct for want of an account of the photoelectron cross sections. Vibrational effects are taken into account only qualitatively, and no attempt has been made yet to reproduce the actual vibrational envelopes. The spectral bands of the silatranes can be affected by vibronic coupling effects. Such an effect should be important here due to the large coupling constant for certain modes and the presence of degenerate ^{2}E electronic states subject to Jahn−Teller effect. Finally, one should not neglect a possible error in the ground-state geometry, which was computed using a still rather modest 6-31G* basis set. In the view of all these factors, the agreement of the theoretical and experimental spectral profiles can be considered to be satisfactory.

Aspects of Si ← N Bonding. Much useful information on electronic structure and bonding can be gained by studying various trends in the molecular ionization energies. The strong dependences of the N 2p LP and Si−X IEs on the Si−N separation in H− and Me−silatranes, which were established in the present study, are especially interesting.

In Figure 5, we show the results of our OVGF calculations for the lowest five IEs in H− and Me−silatranes as a function of the Si−N distance. The calculations were performed for seven

(40) (a) Schirmer, J.; Cederbaum, L. S.; Walter, O. *Phys. Rev. A* **1983**, *28*, 1237. (b) Schirmer, J.; Angonoa, G. *J. Chem. Phys.* **1989**, *91*, 1754. (c) Schirmer, J.; Trofimov, A. B.; Stelter, G. *J. Chem. Phys.* **1988**, *109*, 4734.

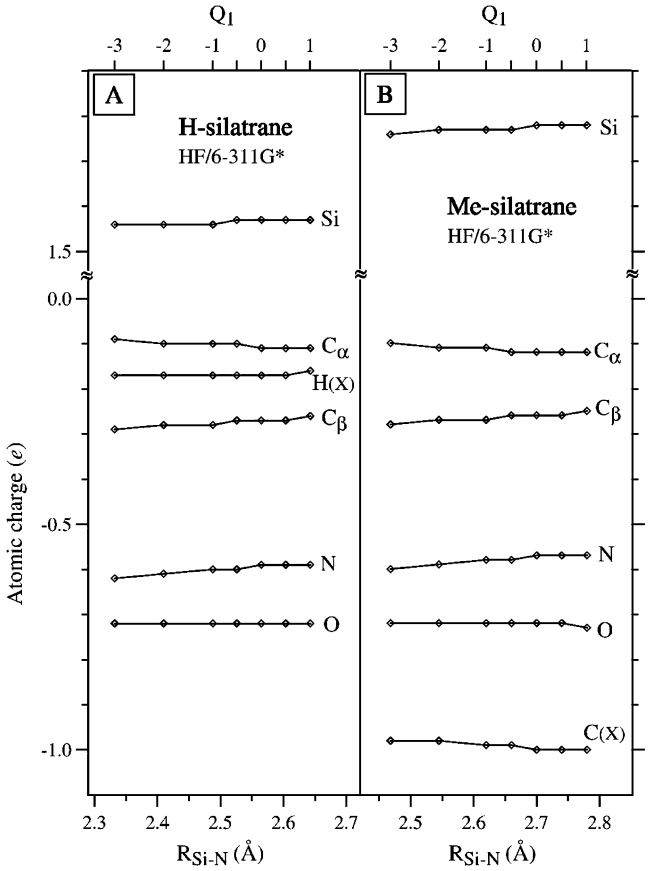

Figure 6. HF Mulliken atomic charges in hydro−silatrane (A) and methyl−silatrane (B) as functions of the Q_1 normal coordinate describing variation of the Si−N distance.

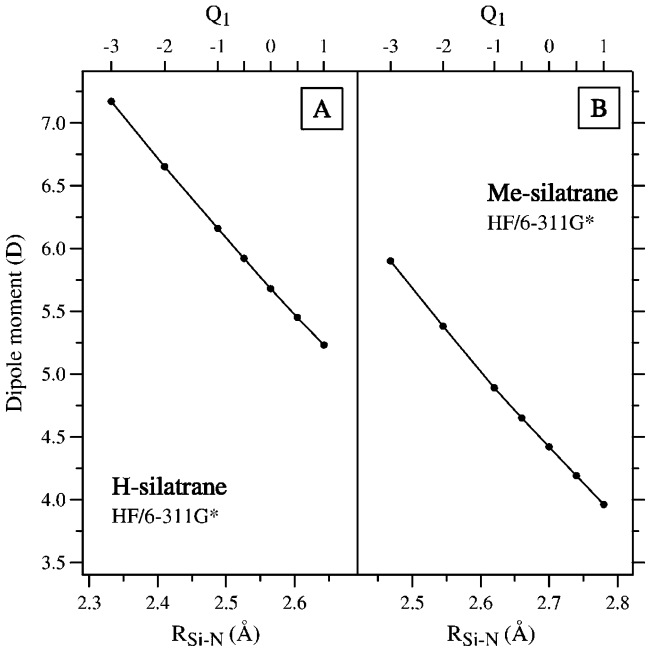

Figure 7. HF ground-state dipole moment of hydro−silatrane (A) and methyl−silatrane (B) as functions of the Q_1 normal coordinate describing variation of the Si−N distance.

values of the normal coordinate Q_1 ($-3 \leq Q_1 \leq 1$), which correspond to Si−N distances within the range 2.3−2.6 Å in H−silatrane and 2.5−2.8 Å in Me−silatrane. The IE curves in the two molecules look qualitatively similar and behave essentially as predicted in the section "Geometrical Dependence of Ionization Energies" of this paper. As the Si−N separation grows, the IE of the N 2p LP levels rapidly decreases, whereas the IE of the Si−X MOs increases. Previously, the dependence of these orbital energies on the Si−N separation (measured by the extent of pyramidalization on the N atom) was studied at the semiempirical MNDO and qualitative model levels, but somewhat different curves were obtained.[11] In contrast to the IEs of the N 2p LP and Si−X MOs, the IEs of the O 2p levels remain relatively constant. Since the observed variations of the IEs are obviously related to changes in the molecular electrostatic potentials and electronic structure, in Figures 6 and 7, we study the behavior of the atomic charges and ground-state dipole moments in H− and Me−silatranes with respect to the Si−N distance. Here, we make use of the HF results for the same Q_1 points as above and employ Mulliken population analysis to estimate the charges on the Si, N, C_α, C_β, and O atoms.

Atomic charges in both molecules remain remarkably constant within the whole range of the Si−N distances considered in Figure 6. This is especially surprising in view of the substantial structural rearrangements that take place in the molecules as the Si−N separation increases. That the electron populations of the Si and N atoms do not change as the atoms separate indicates that there is no appreciable electron density redistribution (or charge transfer) between them since, otherwise, one would observe an increase of the negative charge on N and of the positive charge on Si. Such a situation is possible only if there are no strong orbital interactions between the Si and N atoms. This is indeed the case since HF calculations find only insignificant mixing of the Si and N atomic orbitals (AO) in the N 2p LP and Si−X MOs, with no clear bonding or antibonding pattern. Only localized orbital analysis performed for the HF canonical MOs suggests weak covalent Si−N and Si−X σ-bonds are present,[15−17,22,23] in agreement with the predictions of 3c4e and dative interaction models.[5,6]

The ground-state dipole moments (μ) in both molecules are represented by almost perfectly linear functions which rapidly decrease as the Si−N separation grows, in agreement with previous theoretical studies.[3,18] Within the interval of 0.3 Å, the dipole moments decrease by about 2.0 D (from 7.2 to 5.2 D in H−silatrane and from 5.9 to 4.0 D in Me−silatrane). Here, the linear character of μ is clearly related to the invariance of the atomic charges, q, with respect to the Si−N distance. According to the definition $\vec{\mu} = q\vec{l}$, the dipole moment is indeed a strictly linear function of the distance l if q is constant. Since the atomic charges in H− and Me−silatranes are quite similar (panels A and B of Figure 6), the μ functions have nearly the same slopes in these molecules. At first glance, it might be surprising that μ decreases as the Si−N distance increases (one may expect the opposite behavior of μ, assuming that it is determined chiefly by the Si and N atomic charges). In reality, since the charges on the other atoms, such as oxygens, are also important, the center of gravity of the negative charge is located near the Si site of the molecule, whereas the center of the positive charge finds itself closer to the N atom. This results in a μ vector, which is directed from Si to N, that is opposite to the one expected from the Si and N charges alone. As the Si−N

distance increases, the centers of the negative and positive charges move toward each other, and the dipole moments decrease.

Having established the absence of appreciable Si−N orbital bonding and an important role for electrostatic effects, we may return to the discussion of the ionization energy curves in Figure 5. Here, we note that the present OVGF curves closely reproduce those obtained at the HF level (not shown in Figure 5). The OVGF results are simply shifted by about 1.4−1.6 eV to lower energy (see also Tables 5 and 6). Electron correlation therefore does not change qualitative trends in the electron density and charge distribution, which were established above at the one-particle level of approximation. The present correlated calculations also do not support the picture of an intramolecular Si ← N charge transfer in silatranes.

To make the latter point more obvious, we recall that in the Si ← N charge-transfer model, one assumes a transfer of the N 2p LP electron density into virtual MOs localized on the Si atom. According to the Mulliken classification of donor−acceptor interactions, this is so-called $n\sigma$- or $n\nu$-type of bonding.[41] The latter has essentially multiconfigurational character as it requires mixing of the HF ground-state (GS) with configurations characterized by the excitation of N 2p LP electrons into (Si-localized) virtual MOs. In the silatranes, such configuration mixing is unlikely for several reasons. First, the excited configurations here are energetically too high for an efficient interaction with the GS. This can be seen already from the large gap (of more than 14 eV in the present calculations) separating the highest occupied and lowest unoccupied MOs. Moreover, there is no compact, Si-localized virtual MO that could induce significant configuration mixing with the N 2p LP MO.

All of these considerations are directly confirmed by our preliminary configuration interaction (CI) calculations and calculations using the third-order algebraic−diagrammatic construction [ADC(3)] electron propagator method.[25,40] The CI calculations describe the electronic GS of the two molecules as being dominated by the HF configurations and predict no low-lying excited states. The ADC(3) calculations essentially reproduce the OVGF results for the outer-valence region and find no low-lying shake-up or shake-down satellites, which could be interpreted as signatures of charge-transfer effects.[42] Finally, we note that one should not confuse the (multiconfigurational) intramolecular charge transfer discussed above with the redistribution of electron density due to formation of a (weak) covalent Si−N bond, which is also often referred to as charge transfer in silatrane literature.

The present results demonstrate the importance of electrostatic effects for ionization energies and Si ← N bonding in H− and Me−silatrane molecules. Electrostatic interactions are among the most common stabilization mechanisms in donor−acceptor complexes.[43] A recent X-ray diffraction study of the electron density in Me−silatrane has shown that the electron distribution in the Si ← N interaction region conforms to a so-called closed-shell interaction with a very small covalent contribution, and that the Si ← N bond most likely has an electrostatic nature.[14] Thus, the behavior of the N 2p LP and Si−X MO ionization energies with respect to the Si−N distance (Figure 5) can be attributed to the influence of the positively charged environment, which can be conceived as a potential of positive charge acting on the respective electron densities.

Conclusions

In the present work, we have studied theoretically the photoelectron spectra of hydro− and methyl−silatranes (Figure 1). In addition, the molecular geometry and the electronic structure of these systems were investigated in some detail. The vertical ionization energies were computed using the outer-valence Green's function (OVGF) method[25] with the 6-311G** basis set. Some other basis sets ranging from 6-31G* to 6-311G-(2df,p) also were tested in the calculations. The calculations were performed for the equilibrium ground-state (GS) geometries of H− and Me−silatranes optimized with the coupled-cluster single and doubles (CCSD) method[30] and the 6-31G* basis set. To obtain information on the vibrational structure of the photoelectron bands, the linear vibronic coupling (LVC) approach[26] was employed. This allowed us to overcome the limitations of the vertical picture of ionization and rendered useful information for the assignment of the experimental results. The ground-state vibrational frequencies and the normal modes required by the LVC model were computed using the B3LYP model.

Accurate description of the equilibrium Si−N distance is a major challenge in silatrane studies. For this parameter, various well-established theoretical methods yield values which differ by up to 0.3 Å. In this situation, CCSD calculations were undertaken to ensure a reliable description of the molecular geometry. The resulting Si−N distances of 2.39 and 2.52 Å in H− and Me−silatrane, respectively, are in good agreement with the results of the gas-phase measurements.[12,13]

The high flexibility of silatranes along the Si−N coordinate reflects the nature of Si ← N bonding. Our calculations find no appreciable covalent Si−N bonding, and they do not confirm bonding based on intramolecular Si ← N charge transfer. The present results indicate that Si ← N bonding is chiefly electrostatic. The electrostatic nature of Si ← N bonding is confirmed by the invariance of the atomic charges with respect to Si−N distance, by the linear character of the GS dipole moment function, and by the high sensitivity of the ionization energies of the N 2p LP and Si-X levels with respect to the Si−N separation. As the Si−N distance grows, the binding energies of the N 2p LP electrons decrease, while those of the Si−X IEs increase. These trends in IEs can be explained by changes in the local positive electrostatic potentials near the N 2p LP and the Si−X bond.

The strong geometrical dependence of the N 2*p* LP and some other ionization energies implies strong relaxation of the molecular structure upon ionization and an increased vibrational width of the corresponding photoelectron bands. The presently evaluated vibrational widths of the N 2p LP levels (0.79 and 0.71 eV for H− and Me−silatrane, respectively) imply very broad bands.

The theoretical spectra simulated by combining vertical ionization energies with vibrational widths of the individual transitions agree qualitatively with experimental results and

(41) (a) Mulliken, R. S. *J. Am. Chem. Soc.* **1952**, *74*, 811. (b) Mulliken, R. S. *J. Phys. Chem.* **1952**, *56*, 801. (c) Mulliken, R. S.; Person, W. B. *Molecular Complexes*; Wiley-Interscience Publishing: New York, 1969.
(42) Trofimov, A. B.; Breidbach, J.; Schirmer, J. In preparation.
(43) For example, see: (a) Kaplan, I. G. *Theory of Molecular Interactions*; Elsevier: Amsterdam, 1986. (b) Guryanova, E. N.; Goldshtein, I. P.; Romm, I. P. *Donorno-akceptornaya svias*; Khimiya: Moscow, 1973.

allow for reliable assignments of the observed spectra (Figures 3 and 4). The important advantage of the present approach is that it predicts the shape of the spectral envelope, thereby verifying tentative assignments. In particular, this was quite useful in the characterization of the energetically lowest band, which has the appearance of a distinct, broad maximum in Me−silatrane and of a shoulder in H−silatrane. The present results allow one to unambiguously assign these bands to the N 2p LP ionization transitions. According to our findings, the broad shape of the bands reflects strong vibrational excitations (mainly of the Si−N stretching modes) accompanying detachment of the N 2p LP electrons. The calculated photoelectron spectra allow for a clear assignment of at least three more bands in the observed spectra. The B peaks in both cases are built of two transitions representing ionization from the O 2p LP levels. The C peaks comprise transitions representing ionization from an O 2p LP level and ionization from a Si−X orbital. The D maxima have more complex structure, comprising one transition due to ionization from an O 2p LP level and transitions representing ionization of deeper σ-levels.

It may be interesting to study the photoelectron spectra of silatranes with different X substituents (X = F, OMe, and so forth) using the same theoretical approach. Such a study should enable verification of suggestions concerning the electrostatic character of Si ← N bonding, as formulated in the present work, and would provide material for the analysis of substituent trends in electronic structure and spectra of silatranes.

Acknowledgment. The authors are indebted to Professor Jochen Schirmer for careful reading of the manuscript and numerous valuable suggestions. The authors are also grateful to Professor B. A. Trofimov for his interest in this work and stimulating discussions. This work was supported by a National Science Foundation grant (CHE-0135823) to Kansas State University and by Grants RFBR 02-03-32500, RFBR 02-03-33182, and INTAS 03-51-4164.

JA045667Q